Digital Object Identifier 10.1109/LMWC.2022.3205425

IEEE Microwave and Wireless Technology Letters

Highly Selective Broadband mm-Wave Diplexer Design

Chad Bartlett
Oleksandr Glubokov
Fynn Kamrath
Michael Höft

Suggested Citation

C. Bartlett, O. Glubokov, F. Kamrath and M. Höft, "Highly Selective Broadband mm-Wave Diplexer Design," in IEEE Microwave and Wireless Technology Letters, vol. 33, no. 2, pp. 149-152, Feb. 2023.

Highly Selective Broadband mm-Wave Diplexer Design

Chad Bartlett, Oleksandr Glubokov, Fynn Kamrath, and Michael Höft

***Abstract*—This letter presents a novel broadband diplexer design that is capable of achieving highly stringent rejection characteristics though the use of singlets whose interconnecting irises are formulated as resonant slot-irises. The combination of these two resonant-cavity types allows for a unique filtering solution with increased filter order, wide available bandwidth, low geometric complexity and simple milling requirements which can be suitably applied to millimetre-wave and submillimetre-wave applications. A prototype is fabricated for operation in the W-band (75 GHz - 110 GHz) in order to cover a 10% fractional bandwidth in each passband. Measurement of the prototype denotes highly accurate results and exemplifies the use of all resonator and coupling elements in order to support ten poles and four transmission zeros in an elegant diplexer solution.**

***Index Terms*—Diplexer, filter design, resonant iris, singlet.**

I. Introduction

AS ELECTROMAGNETIC spectrum allocations become more crowded within the microwave frequency regions, the millimetre and sub-millimetre wave regions become more attractive for future large-scale applications such as the internet-of-things (IoT) and radar/satellite remote sensing. One difficulty in the commercialization of instruments and systems beyond the microwave region has been the ability to reliably and easily produce components at scale. In the case of filter networks, work such as [1]–[4] have demonstrated concepts that enable stringent or complex filter characteristics with the use of advanced techniques that enable simple milling procedures for high-precision micromachining. However, for satellite applications to reach highly stringent rejection characteristics through the use of transmission zeros, bypass/cross-couplings and dual-mode filters/diplexers are commonly used – [5]–[8] – ultimately avoiding the folding of resonator structures which are typically required to achieve physical cross-coupling dependencies. This is especially important when considering the layout of high-end manifold diplexers and multiplexers. The use of these type of dual-mode filters has been well demonstrated throughout the K-band regions, however, drawbacks in the production of this type of filter usually stems from challenges while attempting to implement tuning screws or small perturbations, as well as incurring losses due to the misalignment of multi-part assemblies. In order overcome these challenges, we propose a filter layout that is much more suitable for diplexers and multiplexers that are advancing toward use in the terahertz regime.

Manuscript received XX XX, 2022; Revised XX XX, 2022; Accepted XX XX, 2022. This project has received funding from the European Union's Horizon 2020 research and innovation programme under the Marie Skłodowska-Curie grant agreement 811232-H2020-MSCA-ITN-2018. (*Corresponding author: Chad Bartlett.*)

C. Bartlett, F. Kamrath, and M. Höft are with the Department of Electrical and Information Engineering, Kiel University, Kiel 24118, Germany (e-mail: chb@tf.uni-kiel.de; flk@tf.uni-kiel.de; mh@tf.uni-kiel.de).

O. Glubokov is with the Department of Micro and Nanosystems, KTH Royal Institute of Technology, SE-100 44, Stockholm, Sweden (e-mail: glubokov@kth.se).

Color versions of one or more of the figures in this article are available online at http://ieeexplore.ieee.org.

Digital Object Identifier XXX/TMTT.XXXX

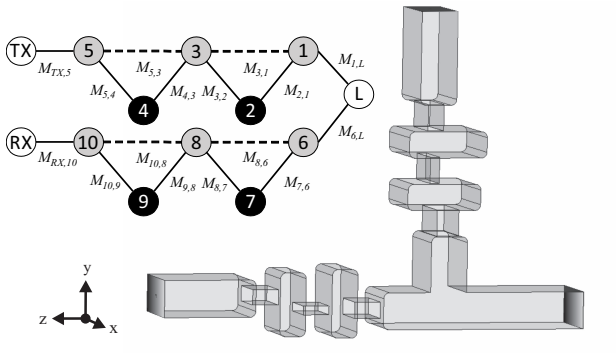

Fig. 1. Vacuum shell and topology of the proposed diplexer scheme where each filtering branch houses two singlets, and three resonant irises. Topology; resonating nodes are black, source/load nodes are white, and gray nodes are resonant slot-irises. Solid lines are direct-coupling paths and dashed lines are bypass-coupling paths. L is common port 1, TX is port 2, and RX is port 3.

To this end, we demonstrate a novel millimetre-wave broadband diplexer that does not require any physical cross-couplings and can be fabricated easily in an E-plane format, where the novelty can be observed in the formation of a quasi-elliptic bandpass response using TM-mode cavities as interconnected singlets while each of the associated coupling irises are formulated as resonating slot-irises. In this manner, an increased filter order, wide available bandwidth, and high selectively is attained in a low complexity solution. The proposed diplexer makes use of two offset back-to-back singlets in each of the filtering branches in order to enable transmission zeros above and below each passband, ultimately allowing for the diplexer's passbands to be placed close together while providing strong rejection at 75 GHz – the bottom end of the W-band – and above 105 GHz. A prototype diplexer is manufactured in brass and demonstrates good measured results, allowing for the novel broadband diplexer to be characterized for the first time within the millimetre-wave regime.

II. Diplexer Design

The design of the diplexer is based on resonant iris and singlet theory presented in [9]–[15]. In [14], a highpass filter scheme was demonstrated through the use of alternating resonant irises and TM110-mode cavities in an inline fashion, while quasi-triplet responses were demonstrated in [15] using triangular cavities with resonant irises. In each of these works [14], [15], transmission zeros are only utilized in the lower end of the passband. In this work however, a modification is proposed in order to convert the highpass response described

$$
\begin{array}{c|cccccccccccc}
 & L & 1 & 2 & 3 & 4 & 5 & 6 & 7 & 8 & 9 & 10 & TX & RX \\
\hline
L & 0 & 0.660 & 0 & 0 & 0 & 0 & 0.632 & 0 & 0 & 0 & 0 & 0 & 0 \\
1 & 0.660 & 0.719 & 0.308 & 0.148 & 0 & 0 & 0 & 0 & 0 & 0 & 0 & 0 & 0 \\
2 & 0 & 0.308 & 0.366 & 0.237 & 0 & 0 & 0 & 0 & 0 & 0 & 0 & 0 & 0 \\
3 & 0 & 0.148 & 0.237 & 0.576 & 0.218 & -0.187 & 0 & 0 & 0 & 0 & 0 & 0 & 0 \\
4 & 0 & 0 & 0 & 0.218 & 0.842 & 0.311 & 0 & 0 & 0 & 0 & 0 & 0 & 0 \\
5 & 0 & 0 & 0 & -0.187 & 0.311 & 0.579 & 0 & 0 & 0 & 0 & 0 & 0.664 & 0 \\
6 & 0.632 & 0 & 0 & 0 & 0 & 0 & -0.765 & 0.263 & -0.157 & 0 & 0 & 0 & 0 \\
7 & 0 & 0 & 0 & 0 & 0 & 0 & 0.263 & -0.405 & 0.200 & 0 & 0 & 0 & 0 \\
8 & 0 & 0 & 0 & 0 & 0 & 0 & -0.157 & 0.200 & -0.631 & 0.210 & 0.138 & 0 & 0 \\
9 & 0 & 0 & 0 & 0 & 0 & 0 & 0 & 0 & 0.210 & -0.824 & 0.293 & 0 & 0 \\
10 & 0 & 0 & 0 & 0 & 0 & 0 & 0 & 0 & 0.138 & 0.293 & -0.627 & 0 & 0.628 \\
TX & 0 & 0 & 0 & 0 & 0 & 0.664 & 0 & 0 & 0 & 0 & 0 & 0 & 0 \\
RX & 0 & 0 & 0 & 0 & 0 & 0 & 0 & 0 & 0 & 0 & 0.628 & 0 & 0
\end{array}
\quad \text{(CM.1)}
$$

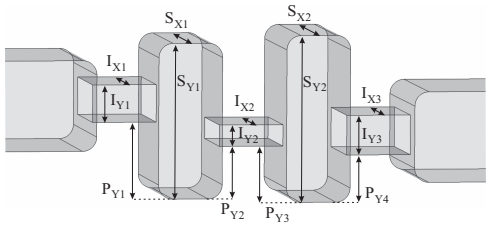

Fig. 2. Close-up view of a vacuum shell for the bandpass filters in each of the diplexer's filtering branches. Dimensions are given in Table 1.

TABLE I. Diplexer Branch Dimensions (in mm).

Dimension†	Filtering Branch RX	Filtering Branch TX
I_{X1}	1.620	1.996
I_{X2}	1.556	1.844
I_{X3}	1.618	1.908
I_{Y1}	0.526	0.770
I_{Y2}	0.300	0.322
I_{Y3}	0.558	0.556
S_{X1}	2.184	2.568
S_{X2}	2.339	2.738
S_{Y1}	2.184	2.568
S_{Y2}	2.339	2.738
P_{Y1}	1.062	1.115
P_{Y2}	0.714	0.867
P_{Y3}	0.763	0.865
P_{Y4}	0.635	0.748

†Dimensions are rounded to three decimal places. Radii and element lengths are 0.2 mm and 0.9 mm, respectively.

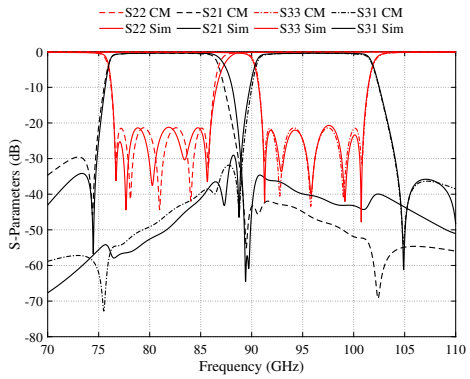

(a)

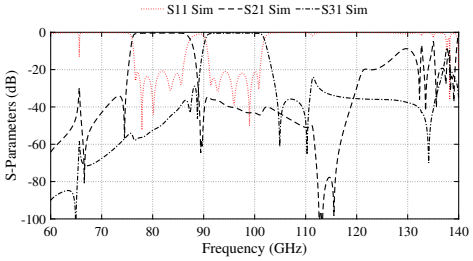

(b)

Fig. 3. (a) Coupling matrix (CM) profile and simulated S-parameters of the proposed diplexer. Q_u is taken as 550 and the equivalent conductivity is taken as 15.9 MS/m, and (b) The simulated spurious performance over a wide range.

in [14] to a quasi-elliptic bandpass response by offsetting one or more of the singlet's feeding ports. This effectively modifies the topology to support a quasi-elliptic bandpass characteristic by forcing a transmission zero response into the upper frequency range of a selected highpass response while simultaneously benefiting from the additional poles and coupling strength provided by the resonant irises. The resulting bandpass filter's attributes are highly desirable when considering the reduced complexity, size compaction and stringent transmission zero response that can be realized without the need of physical cross-couplings or complex assembly. In this format, the structure can be optimized to obtain the required passband specifications through proper positioning of the singlet's feeding ports [12], [13]. Design equations can be followed from [16], [17], while an approximation for the resonant-irises follows from [11], [18] as

$$f_{res\_iris} = \frac{c}{2 \cdot I_x}. \quad (1)$$

As an example case, we propose a novel diplexer design where each filtering branch is capable of producing five poles and two transmission zeros by setting two TM110 singlets back-to-back and configuring the standard coupling irises as resonant-slot type irises. To demonstrate stringent characteristics, the lower passband transmission zero is set to reach a rejection level of 20 dB at the lowest end of the W-band (75 GHz), while simultaneously obtaining a 20 dB passband starting at 76.5 GHz. Each of the passbands are set for a broadband response that covers more than 10% fractional bandwidth (FBW). The upper passband is set very close to the lower one; the 3 dB spacing is approximately 2.7 GHz and the start of the upper passband is approximately 91.2 GHz.

An outline of the proposed diplexer unit is depicted in Fig. 1 in its vacuum-shell form along with its corresponding topology where the transmit port (TX; port 2) will serve as the lower frequency passband, and the receive port (RX; port 3) will serve as the upper frequency passband. The diplexer is realized by routing two filter branches with a T-junction in an E-plane format. Notably, the design complexity of each branch is kept low and suitable for fabrication beyond the millimetre-wave region. Fig. 2 depicts a close-up view of a filter-branch scheme in its vacuum-shell form; the dimensions are detailed in Table 1 for each of the diplexer's branches. The coupling matrix profile (CM.1) and the simulated S-parameters of the diplexer that is outlined in Fig. 1 and Table 1 are given in

TABLE II. Sample Comparison of State-of-the-Art Diplexers in Relative Frequency Bands.†

f_c	FBW	Tech.	Design Elements	Response	IL (dB)	RL (dB)	Ref. (year)
73.5 / 83.5	8.80% / 7.80%	DRIE	Direct coupled	Chebyshev	<0.7* / <0.7*	>13 / >14	[19] (2016)
131 / 143.1	3.28% / 5.66%	DRIE (RFS)	Direct coupled	Chebyshev	1.2* / 0.8*	>20 / >18	[20] (2020)
129 / 150	3.00% / 2.60 %	MLS	Coupled/mixed inverter	Chebyshev	4.2* / 4.5*	>8 / >10	[21] (2021)
97.5 / 105.4	5.62% / 4.99%	HP-Milled	Coupled/mixed inverter	Freq. Dependent	0.34-0.76 / 0.55-0.88	>21 / >21	[4] (2021)
73.5 / 83.5	9.52% / 8.38 %	HP-Milled	Highpass & Quarter-wave	Freq. Dependent	<1.0* / <1.0*	>21 / >21	[22] (2022)
81.0 / 95.6	11.65% / 10.82%	HP-Milled	Singlet/Resonant Iris	Quasi-elliptic	0.41-0.93 / 0.46-1.28	>18.2 / >14.4	T.W. (2022)

†Table values are estimated as best as possible for the presented measured data where not directly reported. *Measured data is reported as achieved typical values or at center frequency (rather than a range). DRIE = Deep reactive ion etching, RFS = Releasable filling structure, High-precision, MLS = Microlaser sintering, HP = High-precision.

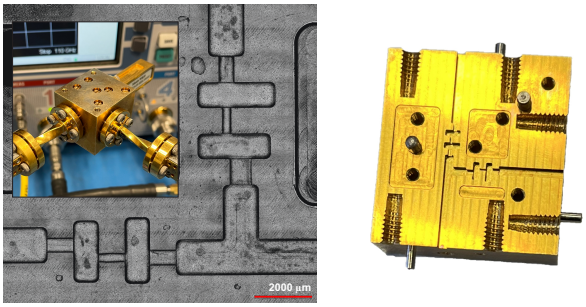

Fig. 4. Laser-microscope image (left) and camera image (right) of the fabricated diplexer along the E-plane. The measured surface roughness S_a is approximately 1 μm. No passivation layer has been applied. The inset of the left image depicts the assembled unit connected to the test-bed.

Fig. 3(a). The singlet's transmission zeros are specified around each passband and allow for close positioning of the passbands to one another while simultaneously providing strong region below 75 GHz and above 105 GHz. The rejection of the lower passband reaches better than 20 dB at 75 GHz and greater than 30 dB at 74.8 GHz. The upper passband rejection reaches better than 30 dB at 104.1 GHz and remains below this threshold throughout the rest of the W-band. Fig. 3(b) is provided as a wideband view of the spurious-mode response from 60 GHz to 140 GHz.

III. Realization, Measurement, and Discussion

For the fabrication of the diplexer, brass has been selected as the cutting material due to its machinability and final surface finish. The prototype is split into two separate blocks along the E-plane for high-precision CNC milling where the radii of both diplexer branches is set to 0.2 mm. The dimensions have been kept to stringent figures to enable precise and accurate milling. For instance, each of the rectangular cavities and resonant-iris lengths have been set to 0.9 mm as detailed in Section II. Fig. 4 depicts the internally milled structures of the diplexer and the fully assembled unit connected to the test-bed.

A comparison of the simulated and measured results are presented in Fig. 5 over 70 GHz to 110 GHz, where 75 GHz is the lower cut-off range of the W-band measurement. This comparison demonstrates good measured results in both pass-bands as well as in the measured rejection regions. The measured return loss is better than 18.2 dB throughout the lower passband and 14.4 dB throughout the upper passband. The measured insertion losses are on the range of 0.41 dB to 0.93 dB and 0.46 dB to 1.28 dB for the lower and upper passbands, respectively, and can be viewed in more detail in the inset image of Fig. 5(a). The measured isolation between

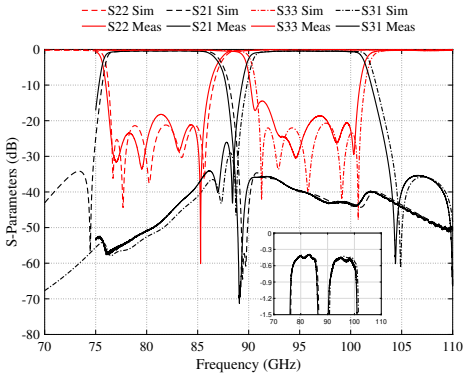

(a)

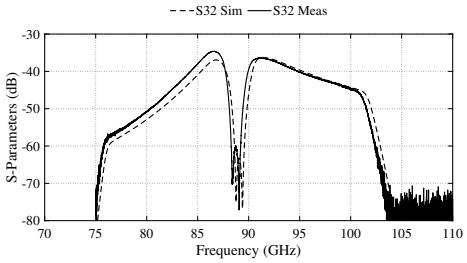

(b)

Fig. 5. (a) Simulated versus measured S-parameters of the proposed diplexer. The inset shows a close-up view of the insertion loss in the lower and upper passbands, and (b) Simulated versus measured isolation between the TX (port 2) and RX (port 3). The equivalent conductivity is taken as 15.9 MS/m.

the transmit and receive ports is provided in Fig. 5(b) and demonstrates an isolation that is better than 34.6 dB near the inner passband edges and drops off to better than 70 dB outside the passband outer edges. Table II is provided as a sample comparison of state-of-the-art diplexers in relative frequency bands, highlighting this work as a compelling design solution with highly competitive results.

IV. Conclusion

A novel broadband diplexer design that is capable of achieving highly stringent rejection characteristics has been presented. The diplexer's filtering branches are formulated by interconnecting two singlets with resonant slot-irises in order to meet a miniaturized design profile with the addi-tional benefits of having increased filter order, wide available bandwidth, low geometrical complexity and simple milling requirements, all without the use of physical cross-couplings. A prototype has been fabricated for operation in the W-band and exemplifies the elegance of the design for potential use in future millimetre-wave and submillimetre-wave applications.

REFERENCES

[1] Y. Xiao, P. Shan, K. Zhu, H. Sun, and F. Yang, "Analysis of a novel singlet and its application in THz bandpass filter design," *IEEE Trans. THz Sci. Technol.*, vol. 8, no. 3, pp. 312–320, Apr. 2018.

[2] D. Miek, et al., "Coupling matrix description of WR-3 waveguide filter with multiple transmission zeros created by source-to-load cross-coupling," *IEEE GeMIC Conf.*, Ulm, Germany, May. 2022, pp. 17-20.

[3] C. Bartlett and M. Höft, "Fully inline and symmetric dual-mode dual-band bandpass filters for millimetre-wave applications," *IEEE MTT-S Int. Microw. Filter Workshop (IMFW)*, Perugia, Italy, Nov. 2021, pp. 323–325.

[4] C. Bartlett, J. Bornemann, and M. Höft, "3-D-Printing and high-precision milling of W-band filter components with admittance inverter sequences," *IEEE Trans. Compon. Packag. Manuf. Technol.*, vol. 11, no. 12, pp. 2140–2147, Sept. 2021.

[5] A.E. Williams, "A four-cavity elliptic waveguide filter," *IEEE Trans. Microw. Theory Techn.*, Vol. 18, No. 12, pp. 1109-1114, Dec. 1970.

[6] A.E. Atia and A.E. Williams, "New types of waveguide bandpass filters for satellite transponders," *COMSAT Techn. Review*, Vol. 1, No. 1, Fall 1971.

[7] H. Ezzeddine, et al., "Compact diplexers and triplexers implemented with dual-mode cavities," Int. J. Microw. and Wireless Technol., vol. 4, no. 1, pp. 51–58, 2012.

[8] B. Yassini and M. Yu, "Ka-Band dual-mode super-Q filters and multiplexers," *IEEE Trans. Microw. Theory Techn.*, vol. 63, no. 10, pp. 3391-3397, Oct. 2015.

[9] J. F. Valencia Sullca, S. Cogollos, V. E. Boria and M. Guglielmi, "Compact dual-band and wideband filters with resonant apertures in rectangular waveguide," *IEEE Trans. Microw. Theory Techn.*, vol. 70, no. 6, pp. 3125-3140, Jun. 2022.

[10] R.-M. Barrio-Garrido, S. Llorente-Romano and M. Salazar-Palma, "Design of Ka band highly selective wideband band-pass filters using directly coupled resonant irises," *IEEE Ant. Prop. Soc. Int. Symp. Dig.*, Columbus, USA, Jun. 2003, pp. 1161-1164.

[11] U. Rosenberg, S. Amari and J. Bornemann, "Mixed-resonance compact in-line pseudo-elliptic filters," *IEEE MTT-S Int. Microw. Symp. Digest*, Philadelphia, USA, Jun. 2003, pp. 479-482.

[12] G. Macchiarella, G. G. Gentili, C. Tomassoni, S. Bastioli, and R. V. Snyder, "Design of waveguide filters with cascaded singlets through a synthesis-based approach," *IEEE Trans. Microw. Theory Techn.*, vol. 68, no. 6, pp. 2308-2319, Jun. 2020.

[13] U. Rosenberg, S. Amari, and J. Bornemann, "Inline TM110-mode filters with high-design flexibility by utilizing bypass couplings of nonresonating TE10/01 modes," *IEEE Trans. Microw. Theory Techn.*, vol. 51, no. 6, pp. 1735–1742, Jun. 2003.

[14] U. Rosenberg, S. Amari, J. Bornemann, and R. Vahldieck, "Compact pseudo-highpass filters formed by cavity and iris resonators," *34th Eur. Microw. Conf.*, Amsterdam, Netherlands, Oct. 2004, pp. 985–988.

[15] C. Bartlett, M. Mehrabi Gohari, O. Glubokov, J. Oberhammer and M. Höft, "Compact triangular-cavity singlet-based filters in stackable multi-layer technologies," *IEEE Trans. THz Sci. Technol.*, Early-view, 2022.

[16] J. Hong, and M.J. Lancaster, "Microstrip filters for RF/microwave applications," *John Wiley & Sons, Inc.*, New York, NY, USA, 2001.

[17] J.-F. Liang, K. Zaki, and A. Atia, "Mixed modes dielectric resonator filters," *IEEE Trans. Microw. Theory Techn.*, vol. 42, no. 12, pp. 2449–2454, Dec. 1994.

[18] J. Uher, J. Bornemann, and U. Rosenberg, *Waveguide components for antenna feed systems: Theory and CAD*, Artech House, Bosten - London, 1993.

[19] V. Nocella, et al., "E-band cavity diplexer based on micromachined technology," *Int. J. Microw. Wireless Technol.*, vol.8, no.2, pp. 179-184 Jan. 2016.

[20] X. Zhao et al., "Silicon micromachined D-band diplexer using releasable filling structure technique," *IEEE Trans. Microw. Theory Techn.*, vol. 68, no. 8, pp. 3448-3460, Aug. 2020.

[21] T. Skaik, et al., "3D Printed microwave components for frequencies above 100 GHz," *IEEE MTT-S Int. Microw. Filter Workshop (IMFW)*, Perugia, Italy, Nov. 2021, pp. 246-248.

[22] F. Teberio, et al., "High-yield waveguide diplexer for low-cost E-band 5G point-to-point radio links," 51st Eur. Microw. Conf., London, United Kingdom, Apr. 2022, pp. 696-699.